Journal of *Marine Science and Engineering*

MDPI

Article

Effect of Hydrodynamic Condition on Adsorption of Sulfadiazine on Marine Sediments

Wei Xu [1,2], Jiaxin Xu [1,2], Jie Song [1,2,*] and Guangli Xiu [1,2,*]

[1] Shanghai Environmental Protection Key Laboratory for Environmental Standard and Risk Management of Chemical Pollutants, School of Resources & Environmental Engineering, East China University of Science and Technology, Shanghai 200237, China
[2] State Environmental Protection Key Laboratory of Environmental Risk Assessment and Control on Chemical Processes, School of Resources & Environmental Engineering, East China University of Science and Technology, Shanghai 200237, China
* Correspondence: jiesong@ecust.edu.cn (J.S.); xiugl@ecust.edu.cn (G.X.)

Abstract: In the present study, the adsorption behavior of sulfadiazine (SDZ) on various sediments under different hydrodynamic conditions generated by a rocking shaker was investigated. Based on the dye mixing experiments, three regimes with different hydrodynamic characteristics, i.e., laminar, transition, and turbulent regimes, were identified. The hydrodynamic intensity was found to have a positive effect on the adsorption of SDZ, In general, the adsorption capacity followed the order of turbulent > transition > laminar > static. Compared to quartz sands, montmorillonite exhibited a narrower range of adsorption capacity under different hydrodynamic conditions, which implies it is less sensitive to the hydrodynamic conditions. For adsorption kinetics, sands fit the pseudo-first-order model, while montmorillonite fits the pseudo-second-order model. For adsorption thermodynamics, the Freundlich model showed a better correlation coefficient for all sediments. In addition, it was found that particle size could affect the antibiotic adsorption capacity, and the presence of salts inhibited the adsorption performance.

Keywords: hydrodynamic condition; sulfadiazine; adsorption; sediments

Citation: Xu, W.; Xu, J.; Song, J.; Xiu, G. Effect of Hydrodynamic Condition on Adsorption of Sulfadiazine on Marine Sediments. *J. Mar. Sci. Eng.* **2023**, *11*, 717. https://doi.org/10.3390/jmse11040717

Academic Editor: Izabela Michalak

Received: 16 February 2023
Revised: 22 March 2023
Accepted: 23 March 2023
Published: 26 March 2023

1. Introduction

Antibiotics have been widely used in the medical, farming, and livestock industries, and antibiotic pollution in the environment has become a critical issue globally. The antibiotic residues in various water environments have been found to range from nanograms to micrograms per liter in surface water and nanograms to micrograms per gram in sediment [1–4]. The residual antibiotics in wastewater will be discharged into the ocean through estuaries, which ultimately leads to a relatively high concentration of antibiotics in the coastal environment [5,6]. It is especially difficult for the antibiotics to be degraded. For example, sulfonamides arecontaminants that can be retained in both coastal water and sediments for a relatively long time [7,8]. Antibiotic residues and their resulting antibiotic-resistant genes also pose an incalculable risk to the ecological cycle of marine microorganisms and human health. Natural selection in the marine water environment can cause the accumulation of bacteria with antibiotic-resistant genes in the environment, producing strains with high levels of drug resistance, and even superbugs, which can cause serious outbreaks of infectious diseases and increased mortality.

A large number of studies have been conducted to examine the adsorption and desorption processes of antibiotics in water and sediment. Li et al. [9] investigated the mechanism and kinetics affecting the adsorption of methamphetamine on marine sediments and simulated the adsorption-desorption behavior of methamphetamine pyrimidine (TMP) in the seawater-sediment system using intermittent stirred flow chamber (SFC) experiments.

Doretto et al. [10] studied the sorption–desorption process of sulfadiazine (SDZ) in a Brazilian soil–water system using intermittent equilibrium experiments. Four types of soils were used for the adsorption of bin and SDZ. Jara et al. [11] investigated the partitioning processes in the water–sediment system of two antibiotics used in farms, flumequine and florfenicol, and they found that the water–sediment partitioning relationship is a key driver of their antibiotic sorption migration. Li et al. [12] studied the hygromycin adsorption process in marine sediments, where they conducted intermittent and stirred flow chamber (SFC) experiments on two marine sediments in order to reveal the kinetic mechanism of the antibiotic adsorption/desorption process. It was found that the adsorption capacity of marine sediments was related to the organic carbon (OC) and fine particle content in the sediments, and different salinity and pH had significant effects on the adsorption performance. These studies mainly focused on the effects of physicochemical properties of the sediment and aqueous environment on the antibiotic migration process. However, the water environment is dynamic in reality, and the effect of hydrodynamic condition on the antibiotic migration process between the water and sediment has not been explored sufficiently.

Previous studies showed that the disturbances induced by wind waves played an important role in the adsorption and desorption process of antibiotics regarding the lake suspended particulate matter. Liao et al. [13] investigated the adsorption and desorption processes of two antibiotics on sediments under the disturbing conditions of wind and waves, and they found that the sediment adsorption capacity of tetracycline and sulfadiazine was significantly enhanced under strong wind conditions. Similarly, Li et al. [14] investigated the process of antibiotic adsorption and migration in the water–sediment interface under simulated wind disturbances by using a stirrer, and they found that both cation exchange capacity and organic matter content affected the adsorption of antibiotics, and the resuspension of sediments promoted the migration transition of antibiotics in the water–sediment interface. Li et al. [15] investigated the kinetics of antibiotic adsorption at the water–sediment interface under the action of wave currents and found that the wave-generated shear force led to a significant increase in the efficiency of antibiotic removal by the lake sediments. Xu et al. [16] investigated the transport and distribution of four antibiotics between coastal water and sediment in both dynamic and quiescent environments by using a lid-driven annular flume, and it was found that there was a more rapid diffusive transfer of antibiotics from water to sediment in the dynamic environment. Previous studies showed that the hydrodynamic condition could affect the adsorption process significantly in the lake environment. However, the effect of hydrodynamic condition on adsorption in the oscillatory coastal environment has not been explored in depth.

In order to better understand the migration process of antibiotics in dynamic coastal environment, the effect of hydrodynamic condition on the antibiotic adsorption behavior between water and sediment was investigated experimentally. In this study, a rocking shaker was used to generate the periodic oscillatory dynamic environment, and the adsorption performance of sulfadiazine (SDZ) on various sediments under different hydrodynamic conditions was examined. Moreover, the effects of particle size and salinity on the adsorption capacity were also analyzed. This study mainly focused on the inorganic components of marine sediments, and the effect of organic components was not considered. This study may help provide a basis to further understand the fate of antibiotics in the estuary and coastal environments.

2. Experimental Methodology

2.1. Setup and Materials

In this study, a rocking shaker (model: Lizhen Technology, RS1) was used to generate the oscillatory flow environment, and the specification of the shaker is shown in Table 1. A transparent acrylic tank with geometry of 280 mm (L) × 150 mm (W) ×200 mm (H) was placed on the shaker platform as the container.

Table 1. Properties of the rocking shaker.

Property	Shaking Frequency (rpm)	Shaking Angle (°)	Platform Dimensions (mm × mm)
Value	10–80	10	360 × 420

Sulfadiazine (SDZ) (purity > 98.0% by weight), purchased from Shanghai Yuanye Biotechnology Co., was applied as the targeted antibiotic. Quartz sands with different particle diameter and montmorillonite (0.075–0.090 mm) were purchased from Shanghai Maclean Biochemical Reagent Co. The marine sediment samples used in the experiments were collected from the Hangzhou Bay, China at the location of longitude 122.330461° E and latitude 29.933766° N. The basic physicochemical properties of the sediments are shown in Table 2. The pH of the sediment was measured by a pH meter. The dry volume weight was obtained by the cutting ring method by weighing 100 mL volume of sediment and calculating the mass difference before and after drying. The water content was calculated by the ratio of the value of the wet volume weight minus the dry volume weight to the wet volume weight. The particle size composition was obtained by the sieving method with 10 mesh and 300 mesh aperture screens, respectively. The organic matter was measured by an organic carbon analyzer. The proportions of C, H, and N elements were obtained by elemental analyzer. The XRD analysis of the sediments was shown in Figure 1. It can be seen that the diffraction spectral peaks of the sediment appear at 2θ = 20.054°, 22.220°, 23.574°, 27.906°, 31.138°, 36.191°, 43.339°, 50.079°, which coincided with the X-ray diffraction of SiO_2 and $CaCO_3$, indicating that SiO_2 and $CaCO_3$ shall be the main components of the sediment samples.

Table 2. Basic physicochemical properties of the marine sediments.

Sediment	pH	Water Content (%)	Dry Volume Weight (g/cm^3)	Particle Size Composition (%)			OM (g/kg)	C (%)	N (%)	H (%)
				Silt Grains (<0.05 mm)	Sand Grains (0.05–2 mm)	Gravel (>2 mm)				
1	7.71	9.53	1.394	1.02	90.91	8.07	0.987	1.19	0.07	0.391

OM, organic matter.

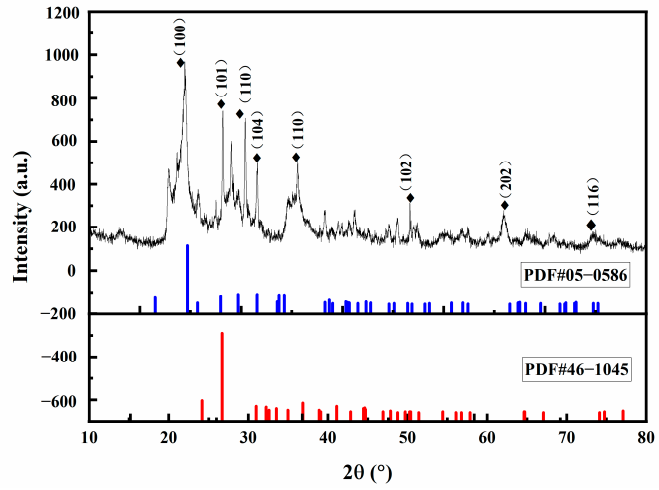

Figure 1. XRD characterization of sediments.

High performance liquid chromatography (HPLC, model: Waters Model 2998) was used to measure the concentration of SDZ. Methanol (99.9% purity, ACS/HPLC grade) and phosphoric acid (Chromatographic grade, 85–90%,) for HPLC measurements were purchased from Beijing Bailingway Technology Co., and Shanghai Aladdin Reagent Co., respectively. Ultrapure water was used for all the experiments. The pH of the water in the

tank in all experiments was maintained at neutral, and the experimental temperature was kept at 25 °C.

2.2. Dye Mixing Experiments

Dye mixing experiments were conducted first to characterize the hydrodynamic conditions in the shaking container. The rocking motion of the shaker produces fluid motions and mixing in the container, and the container was placed on the shaking platform. According to Gardner and Tatterson [17], the Reynolds number *Re* of a rocking shaker was defined as:

$$Re = \frac{NL^2}{\nu} \tag{1}$$

where N is the frequency of shaking, $L = V^{\frac{1}{3}}$, and v is the kinetic viscosity coefficient of the fluid.

Similar to the mixing induced by an impeller, a homogenization number H_o of the rocking shaker was defined to characterize the mixing effectiveness [18,19]:

$$H_o = N\theta \tag{2}$$

where θ is the mixing time. Higher H_o value represents less effective mixing.

In this experiment, tap water was used as the working fluid, and food coloring solution was used as the dye tracer. The density of the dye is approximately equal to that of tap water, and the effects of gravity can be ignored. Different shaker oscillation frequencies ranging from 10 to 60 rpm were used to investigate the effects of oscillation frequency on the mixing time. The dye droplet was added into the fluid with almost no momentum, and the experiment lasted until the dye was homogeneously mixed within the container.

2.3. Antibiotic Adsorption Experiments

In this study, the adsorption behavior of SDZ on marine sediments under various conditions was investigated. The concentration of the SDZ solution ranged from 0.2 to 2 mg/L, and the shaking speed was adjusted from 10 to 60 rpm. During the experiment, the tank was fully covered by a black curtain to eliminate the light effects, certain amounts of sands or montmorillonite were placed on the bottom of the tank, and 1 L SDZ solution with different concentration was added slowly. For the adsorption kinetic experiments, the sample solution was collected at t = 0, 5, 10, 20, 30, 40, 50, 60, 120, 180, and 240 min. The sample was filtered by a 0.45 μm needle filter and then analyzed to measure the concentration. The isothermal adsorption experiments were performed with similar procedure, and the samples with different initial concentrations of SDZ were collected when the adsorption equilibrium was reached at 120 min. HPLC was used to examine the antibiotic concentration by using a C18 reversed-phase column (4.6 × 250 mm, 5 μm). The column temperature was 30 °C. Optimal separation was achieved by isocratic elution of 80% phosphoric acid (0.05%) and 20% methanol. The flow rate was 1 mL/min, the injection volume was 20 μL, and the detection wavelength was 267 nm. The concentration of antibiotic adsorbed on the sediment is obtained by subtracting the detected residual concentration from the initial concentration of the antibiotic, and the amount of adsorbed SDZ can be calculated as follows.

$$Q_t = \frac{(C_0 - C_t)V}{W} \tag{3}$$

where Q_t is the adsorption capacity (mg/kg), C_t is the concentration of sulfadiazine solution at time t (mg/L), C_0 is the initial concentration of sulfadiazine (mg/L), W is the weight of the sediment (kg), and V is the volume of the solution (L).

3. Results and Discussion

3.1. Characterization of Hydrodynamic Conditions by Dye Mixing

In this study, three regimes with different hydrodynamic characteristics were observed: laminar, transition, and turbulent regimes.

When the rocking speed of the shaker was low, i.e., 10–20 rpm, the mixing in the water tank was in the laminar regime. In this condition, there was no deformation of the fluid surface in the tank. When the dye was gently injected into the fluid, it suspended in the fluid and did not disperse quickly, but rather followed the oscillatory movements of the surrounding fluid. Over time, it deformed and dispersed slowly into the fluid. Compared to the other two regimes, the dye droplet in the laminar regime retained its original shape for a relatively long time, and the mixing time of the laminar regime was much longer.

When the shaking speed was higher, i.e., 25–40 rpm, the fluid surface started to deform with a higher frequency of oscillation and surface waves can be observed. Similar to the laminar regime, at the beginning, the dye droplet suspended in the fluid and followed a periodic oscillatory motion with the fluid. However, due to the stronger fluid motion, weak dispersion can be observed as soon as the dye droplet was injected into the fluid. The experimental results showed that the dye droplet diffused into agglomerated flocs under the stronger oscillation and followed the motion of the surrounding fluid. It took a shorter time for the droplet to be mixed homogeneously over the tank.

As the shaking speed kept increasing, i.e., 45–60 rpm, strong turbulence can be observed within the tank. The dye droplet deformed and spread almost immediately once it was injected into the fluid, and only a few seconds were required before the mixing became homogeneous. The turbulent regime produced the strongest mixing, which occurred very rapidly.

The relationship between the mixing time and shaking period is shown in Figure 2. It can be seen that, as the shaking period increases (shaking frequency decreases), the mixing time increases. For the laminar regime, the mixing time ranges from 150 to 310 s. In this regime, decrease in the shaking period can shorten the mixing time significantly. For transition regime, the mixing time is shorter than that in the laminar, ranging from 6 to 26 s. For the turbulent regime, the mixing is the most explosive, and the mixing time is within a few seconds.

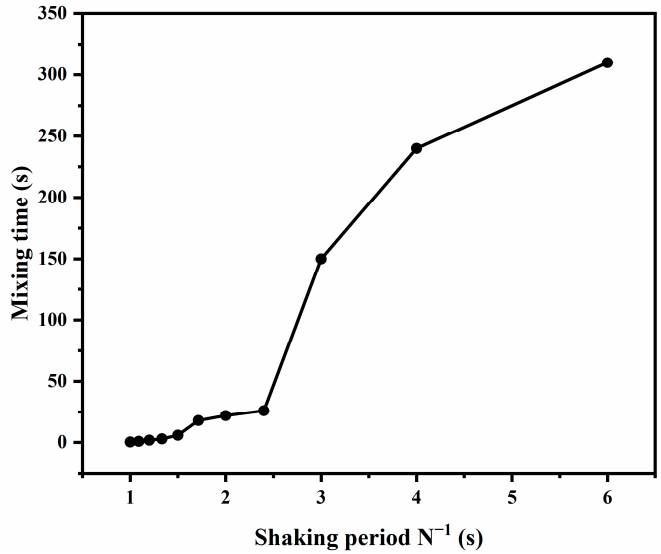

Figure 2. Relationship between mixing time and shaking period.

Figure 3 demonstrates the relationship between the Reynolds number and homogenization number. The homogenization number also clearly showed the three different regimes, which coincided with the previous results. It can be seen that, when *Re* ranged from 1667 to 3333, *Ho* was maintained at a relatively high value, i.e., above 50. In this

regime, *Ho* even increased as *Re* increased. The reason is that *Ho* is the product of the shaking frequency and mixing time, and, when the mixing is fairly weak, a higher frequency may not reduce the mixing time quickly. The reduction in mixing time is slower than the increase in the shaking frequency, and this leads to an increase in *Ho*. When *Re* ranged from 4167 to 6666, the flow entered the transition regime. In the transition regime, the effect of *Re* on *Ho* was negligible, where *Ho* retained almost a constant of 10 as *Re* increased, which implies that an increase in the shaking speed will not affect the mixing effectiveness. As *Re* increased further, the value of *Ho* dropped rapidly. In the turbulent regime (i.e., *Re* > 7500), *Ho* decreased with *Re*, which suggests that the mixing is more effective, and the enhanced frequency can lower the mixing time considerably.

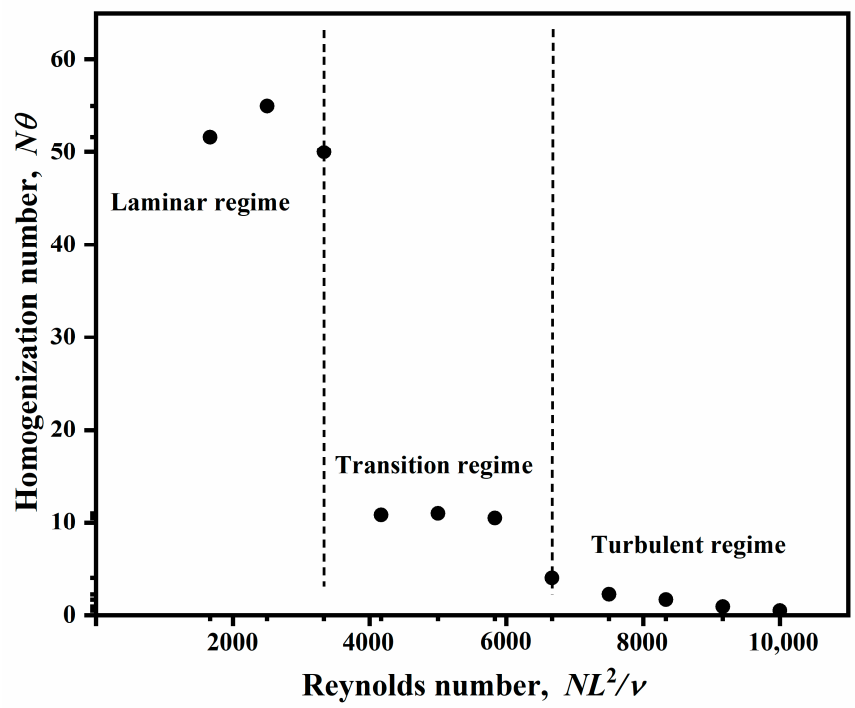

Figure 3. Relationship between Reynolds number and homogenization number.

3.2. Effect of Hydrodynamic Condition on SDZ Adsorption

The adsorption performance of sulfadiazine on various sediments under different hydrodynamic conditions was investigated, as shown in Figure 4. The Reynolds number ranged from 1677 to 9166 with three types of sediments being used: coarse sand (2–3 mm), fine sand (250–425 μm), and montmorillonite. It can been seen that the adsorption amount increased rapidly from 0 to 60 min. Thereafter, the increase became slow, and the adsorption reached the steady state at about 120 min for all cases.

Figure 4 shows that the adsorption behavior under different hydrodynamic conditions varies significantly, which implies that the hydrodynamic condition plays an important role on the antibiotic adsorption. As the *Re* increased, the adsorption amount increased generally. For coarse sand and montmorillonite, as *Re* increased from 1677 to 9166, the adsorption amount increased from 2.211 mg/kg to 5.548 mg/kg and 1.362 mg/kg to 2.051 mg/kg, respectively. Fine sand exhibited the maximum adsorption in the transition regime, which was 3.846 mg/kg. The reason could be that higher *Re* induces more intensive hydrodynamic environment, which leads to more extensive contact between the sediments and fluid, and thus more antibiotic could be adsorbed by the sediments.

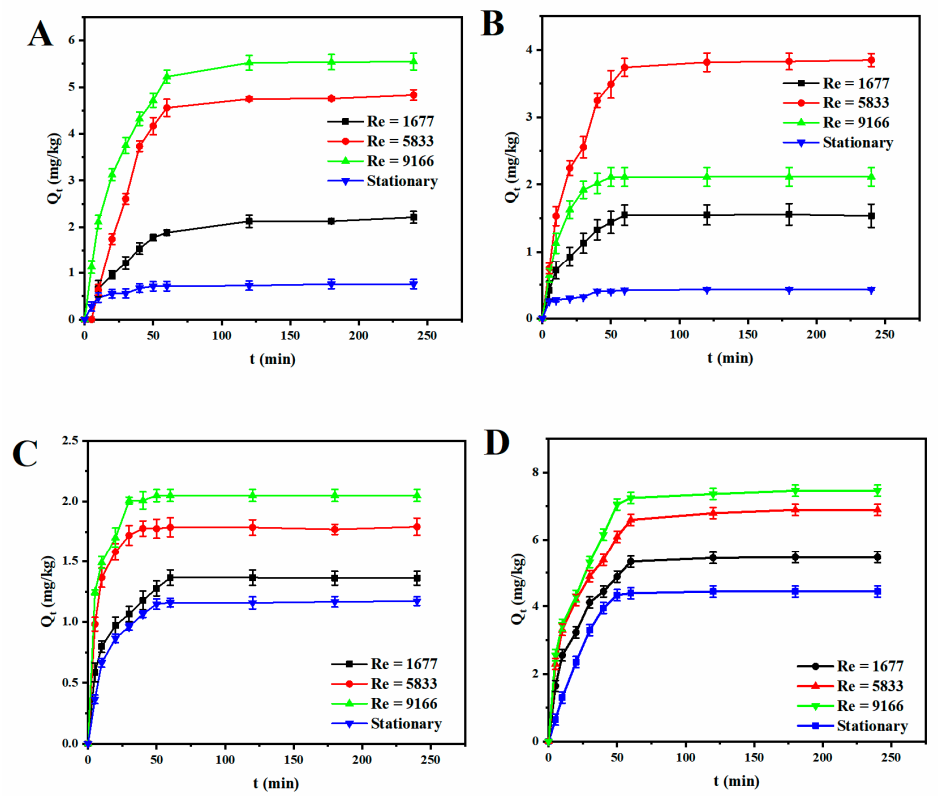

Figure 4. Variation of adsorption amount with time under different regimes on (**A**) 2–3 mm quartz sand (**B**) 250–425 μm quartz sand (**C**) montmorillonite and (**D**) sediment sample.

By comparing the adsorption behavior of different sediments under the same hydrodynamic condition, it was found that the adsorption capacity of the sediment sample >2–3 mm sand > 250–425 μm sand >montmorillonite in the dynamic environment. This finding is similar to that of Kim et al. [20], who classified particle size into sand, silt, and clay with the aim of finding out the effect of particle size of sediment on fluoride adsorption and found that particles with larger diameters had higher adsorption capacity for fluoride. However, when the fluid was static, montmorillonite showed an adsorption capacity of 1.172 mg/kg, which was higher than both coarse and fine sands. In this study, the adsorption of SDZ on montmorillonite was found to be smaller than that of tetracycline and ciprofloxacin antibiotics, where montmorillonite showed a stronger adsorption capacity [21]. Tetracycline and ciprofloxacin are molecules in a positively charged ionized state, while sulfadiazine is generally negatively charged at pH values greater than 4, which limited its adsorption on montmorillonite. It also can be seen that, for coarse and fine sands, the adsorption amount varied significantly as the Reynolds number increased from static to the turbulent regime. For 2–3 mm sand, the adsorption amount was enhanced by 7.3 times. Additionally, the adsorption capacities of coarse and fine sands changed in opposite ways when the Reynolds number was changed from 5833 to 9166. To the contrary, the effect of hydrodynamic condition on the adsorption behavior of montmorillonite was relatively small. As *Re* increased from 0 to 9166, the adsorption amount was only increased by 1.75 times. This suggests that montmorillonite tends to be less sensitive to antibiotics adsorption than to the changes in hydrodynamic conditions. This could be attributed to the different physicochemical properties between sands and montmorillonite. Montmorillonite has smaller particle diameter, as well as lower density. Hence, it is easier to be mixed well with the fluid even when the hydrodynamic condition is relatively weak. While, for sands, the hydrodynamic condition plays a more important role on the particle resuspension and mixing, and it leads to more variable results [22,23]. It can be seen in Figure 4D that the adsorption capacity of marine sediment samples was slightly greater than that

of coarse sands, regardless of the hydrodynamic conditions, which is consistent with the physiochemical properties of the sediment samples. In addition, the presence of organic matter in the real sediments promoted the adsorption of antibiotics, which led to a higher adsorption capacity.

To analyze the adsorption kinetic mechanism, the experimental results were fitted by the pseudo-first-order (PFO) and pseudo-second-order (PSO) models, as shown in Table 3. The models can be expressed by:

$$ln(q_e - q_t) = lnq_e - k_1 t \quad (4)$$

$$\frac{t}{q_t} = \frac{1}{k_2 q_e^2} + \frac{1}{q_e} t \quad (5)$$

where k_1 (min^{-1}) and k_2 ($kg \cdot mg^{-1} \cdot min^{-1}$) are the adsorption rate constants of the PFO and PSO kinetic models, respectively, and q_t and q_e are the amount of antibiotic adsorbed per unit mass of sediment at moment t and at equilibrium (mg/kg), respectively [24].

Table 3. Adsorption kinetic parameters of PFO and PSO models of SDZ adsorption on different sediments.

Sediments	*Re*	q_e (mg/kg)	PFO			PSO		
			$q_{e,cal}$	k_1	R^2	$q_{e,cal}$	k_2	R^2
2–3 mm	1677	2.121	2.080	0.0361	0.994	2.390	0.0188	0.933
	5833	4.912	5.001	0.0286	0.992	5.118	0.0071	0.921
	9166	7.073	7.291	0.0281	0.967	7.317	0.0038	0.916
250–425 μm	1677	1.659	1.622	0.0411	0.992	1.842	0.0289	0.956
	5833	3.779	3.709	0.0472	0.971	4.127	0.0163	0.935
	9166	2.016	1.951	0.1603	0.984	2.091	0.1246	0.969
Montmorillonite	1677	1.321	1.305	0.0631	0.968	1.451	0.0596	0.978
	5833	1.742	1.718	0.0539	0.972	1.892	0.0427	0.983
	9166	2.016	1.951	0.1603	0.964	2.090	0.1246	0.989
Sediment	1677	5.342	5.296	0.0498	0.982	5.703	0.0118	0.967
	5833	6.771	6.617	0.0505	0.973	7.344	0.0099	0.968
	9166	7.339	7.286	0.0499	0.976	8.080	0.0089	0.957

It can be seen that both models can represent the adsorption process well, i.e., $R^2 > 0.9$. Comparatively, PFO is more suitable for the SDZ adsorption on quartz sands and marine sediment as the R^2 of PFO is slightly higher, which suggests that the adsorption is mainly dominated by physical adsorption. For montmorillonite, the PSO model has a higher R^2 and fits the adsorption process better. This finding is similar to that of Wu [21] et al. who studied the adsorption of tetracycline and ciprofloxacin on montmorillonite and found that the PSO model is more suitable to describe the kinetic process of adsorption of both antibiotics on montmorillonite.

The SDZ adsorption isotherms of different sediments under various hydrodynamic conditions were studied as well. Figure 5 shows the relationship between the equilibrium adsorption capacity and equilibrium concentration at initial concentration of 0.2–2 mg/L. Both the Freundlich and Langmuir models were applied to analyze the experimental results,

$$q_e = K_F C_e^{\frac{1}{n}} \quad (6)$$

$$q_e = q_m \frac{K_L C_e}{1 + K_L C_e} \quad (7)$$

where q_m is the maximum adsorption capacity of the sediment, K_L is the Langmuir isothermal adsorption rate value, and K_F is the Freundlich isothermal adsorption coefficient.

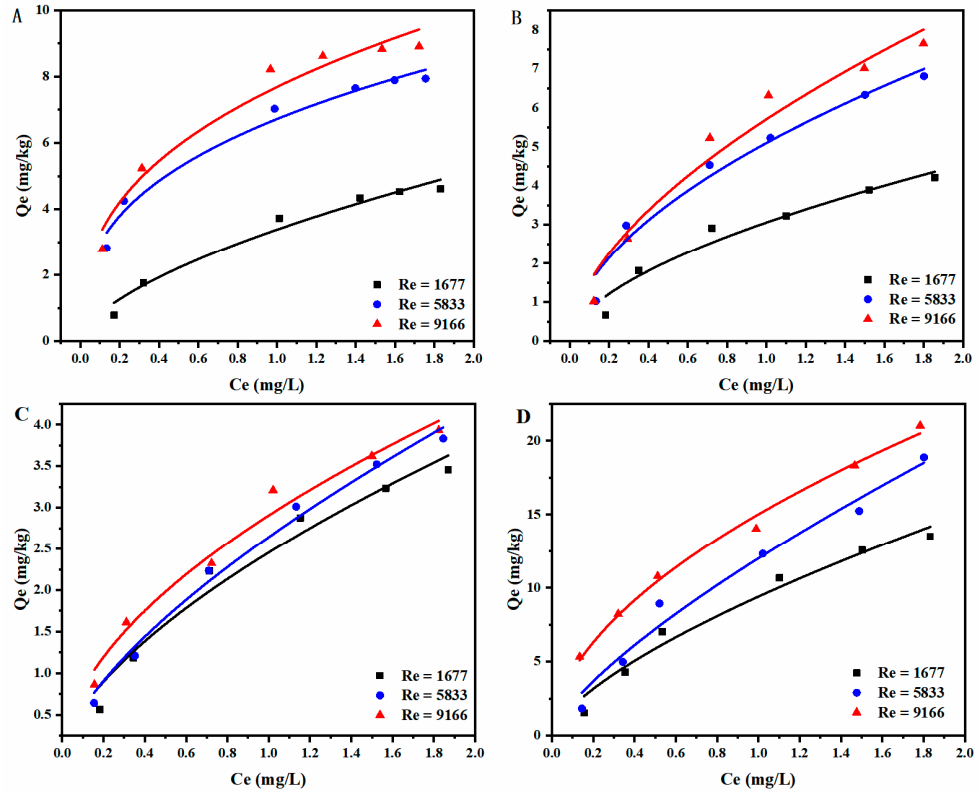

Figure 5. Relationship between equilibrium concentration and adsorption capacity with Freundlich model fitting under different hydrodynamic conditions on (**A**) 2–3 mm quartz sand, (**B**) 250–425 μm quartz sand, and (**C**) montmorillonite. (**D**) Sediment sample.

Figure 5 shows that the antibiotic adsorption capacity increases with equilibrium concentration for all the cases. In general, the equilibrium adsorption capacity of SDZ followed the order of marine sediment >2–3 mm sand > 250–425 μm sand >montmorillonite, which was consistent with the kinetic results. By comparing the adsorption behavior under different hydrodynamic conditions, it was found that larger *Re* tended to generate higher equilibrium adsorption capacity. This shall be attributed to the better mixing performance under stronger turbulent environment [25]. Specifically, the adsorption capacities under transition and turbulent regimes are almost identical for 250–425 μm sand. However, for montmorillonite, the difference between laminar and transition regimes is negligible.

The isotherm model fitting results are demonstrated in Table 4. Both Freundlich and Langmuir models showed good correlation with the experimental results (i.e., $R^2 > 0.9$). However, the R^2 values of Freundlich were slightly higher than that of Langmuir for all types of sediments, indicating that the Freundlich model fit the adsorption behavior better. This suggests that the distribution of active adsorption sites on the sediment surface is not uniform [26]. The q_m of sediment in this study ranged from 25.86 to 41.954 mg/kg. Table 5 shows the maximum sorption capacity (mg/kg) of lake sediments for four different sulfonamide antibiotics in a similar study. From the table, it can be seen that the adsorption capacities of the sediments in this study are all roughly in the same range as the references. Additionally, the Freundlich empirical constant n is greater than 1 for all the cases, implying that SDZ can be easily adsorbed on the sediments. The reason for this nonlinear adsorption result is that, when pH > 6.5, the sulfadiazine molecule is deprotonated and has a neutral or negative charge. The adsorption of SDZ on coarse and fine sands under van der Waals forces exhibits the physical adsorption characteristics. For negatively charged montmorillonite, there is an electrostatic phase repulsion between molecules that affects the adsorption on the particle surface. Therefore, Freundlich is more suitable to describe this nonlinear isothermal adsorption process. Similarly, Akcay et al. [27] found that the Freundlich model was able

to fit the flurbiprofen adsorption on modified montmorillonite well. Bansal's [28] study also showed that the Freundlich adsorption isotherms were better fitted to the adsorption of tetracycline on montmorillonite.

Table 4. Freundlich and Langmuir adsorption parameters of SDZ adsorption on different sediments.

Sediments	*Re*	Freundlich			Langmuir		
		K_F (a)	*n*	R^2	q_m (b)	K_L (c)	R^2
2–3 mm	1677	4.399	1.637	0.982	11.94	0.5317	0.955
	5833	15.187	2.811	0.983	35.73	0.5950	0.958
	9166	13.668	2.669	0.972	12.44	4.6223	0.947
250–425 μm	1677	4.225	1.046	0.982	14.18	0.1127	0.949
	5833	8.896	1.146	0.983	26.33	0.4508	0.959
	9166	7.627	1.242	0.982	17.78	0.6548	0.953
Montmorillonite	1677	3.847	1.018	0.985	27.58	0.0112	0.961

Notes: (a) K_F ($mg \cdot^{1-n} \cdot L^n \cdot kg^{-1}$); (b) q_m ($mg \cdot kg^{-1}$); (c) K_L ($L \cdot mg^{-1}$).

Table 5. Maximum adsorption capacity of lake sediments for four different sulfonamide antibiotics (mg/kg).

Antibiotics	Adsorbents	Maximum Adsorption Capacity q_m (mg/kg)	Reference
SDZ	Lake sediments	26.25	[29]
SM2	Lake sediments	12.76	
SMZ	Lake sediments	8.76	
SDM	Lake sediments	33.90	

In this study, the effect of hydrodynamic conditions on the adsorption performance was investigated by examining the relationship between the hydrodynamic parameter and the adsorption coefficients. Figure 6 shows the variation of kinetic adsorption rate and Freundlich coefficient under different *Re*. For the adsorption kinetics, K_1 is used for quartz sands and marine sediment, and K_2 is used for montmorillonite, as the fitting models are different. Figure 6A showed that the kinetic adsorption rate was maintained as relatively stable at laminar and transition regimes, while it varied significantly at the turbulent regime. This implies that turbulence intensity has a strong effect on the adsorption kinetics. Figure 6B showed the relationship between Freundlich coefficient and *Re*, and, it can be seen that, for montmorillonite, K_F remained almost constant in all regimes, while for sands and marine sediment, the value of K_F increased firstly and then decreased as *Re* increased.

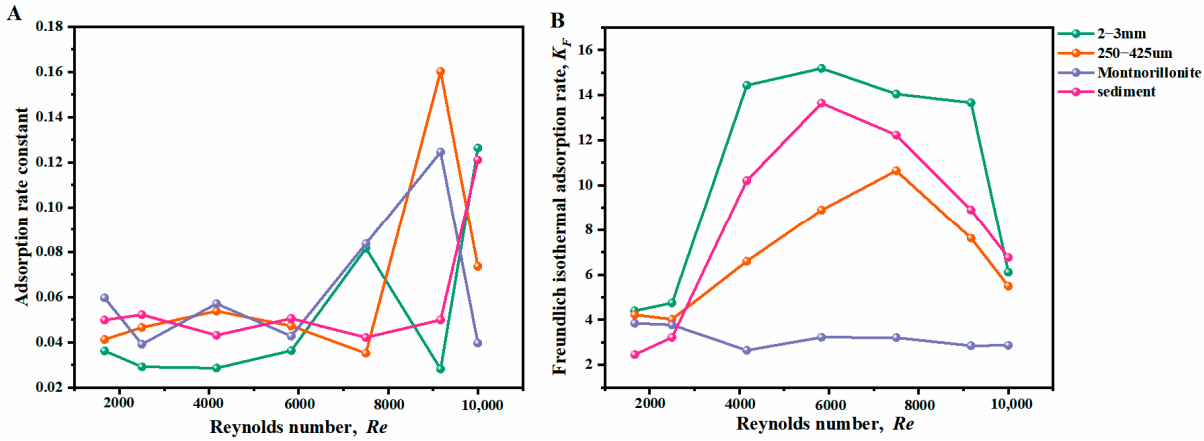

Figure 6. Relationship between Reynolds number and adsorption coefficients, (**A**) adsorption ki–netic constant and (**B**) Freundlich coefficient.

3.3. Effects of Particle Size and Salinity on SDZ Adsorption

Particle size was found that have a strong relationship with the adsorption capacity. Wang et al. [30] found that large particle size can significantly inhibit the adsorption of BPA on the sediments. Buyang et al. [31] also found that fine particles tended to adsorb more lead than coarse particles. Figure 7 shows the equilibrium adsorption amount of different particles under the same hydrodynamic condition. It can be seen that, compared to quartz sands, montmorillonite had the lowest adsorption capacity, which was 2.136 mg/kg. The adsorption capacities of different quartz sands were 5–10 μm > 2–3 mm > 90–106 μm > 1–2 mm > 5–8 mm > 250–425 μm, and the adsorption capacity ranged from 4.758 to 7.420 mg/kg. The results showed that there was no linear relationship between the particle size and adsorption capacity. The greater adsorption capacity of fine sand for antibiotics is attributed to the different interlayer structure [32,33].

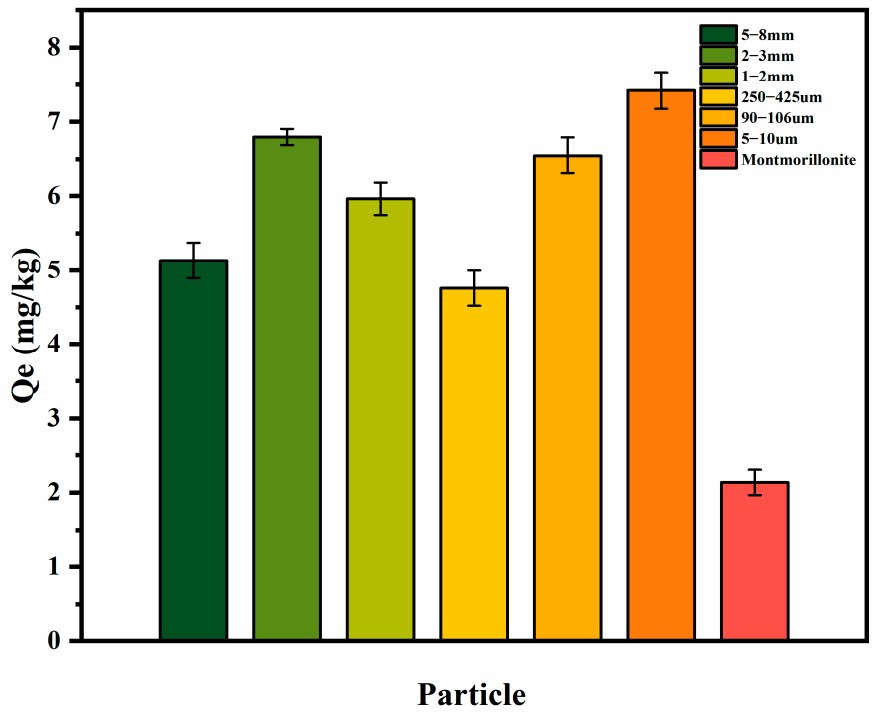

Figure 7. Adsorption capacity of different sediments towards SDZ at *Re* = 7500.

The effects of salinity on the adsorption behavior of SDZ on different sediments were also investigated in this study. Figure 8 shows the adsorption amount of SDZ under various concentration of NaCl at *Re* = 7500. As the salinity increased from 0 to 0.5 mol/L, the adsorption capacity of 2–3 mm and 250–425 μm and montmorillonite and sediment samples decreased from 6.798 to 0.564 mg/kg, 4.758 to 0.397 mg/kg, 1.956 to 0.074 mg/kg and 6.898 to 0.648 mg/kg respectively. It is obvious that the presence of NaCl will inhibit the adsorption of antibiotics, and, the higher the salinity, the smaller the amount of antibiotic that could be adsorbed by the marine sediments [34–37].

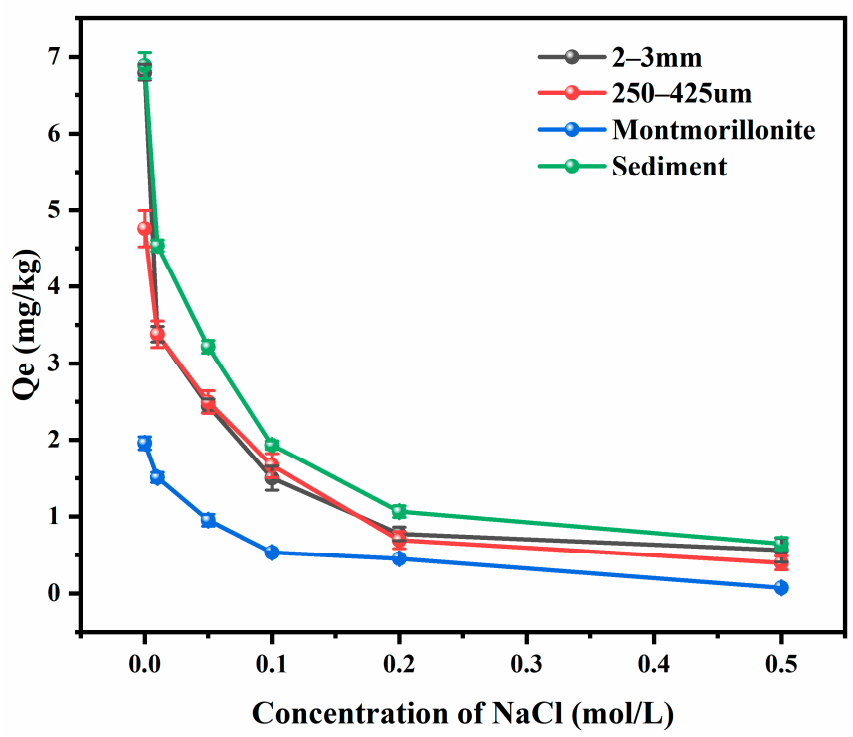

Figure 8. Adsorption of SDZ on different sediments under different salinity at *Re* = 7500.

4. Conclusions

In this experiment, the adsorption process of sulfadiazine antibiotics on common marine sediments under periodic hydrodynamic conditions and the effects of salinity and particle size were investigated. Three hydrodynamic regimes with different characteristics were identified, and the adsorption kinetics and thermodynamics of SDZ under different regimes were studied. It was found that the adsorption capacity varied under different regimes with the order of turbulent > transition > laminar, generally, which shall be attributed to the more intensive contact between the sediments and solution induced by the stronger hydrodynamic condition. In this study, quartz sand and montmorillonite are the main components of the marine sediments collected from Hangzhou Bay. Compared to quartz sands, montmorillonite is less sensitive to changes in the hydrodynamic environment. This is due to the electrostatic repulsion between the negatively charged montmorillonite and the negatively or neutrally charged sulfadiazine molecules, which inhibited the adsorption effect under different hydrodynamic effects. The kinetic adsorption process of quartz sand and marine sediment was mainly based on physical adsorption, while for montmorillonite, the PSO kinetic equation fitted better. Besides, the effects of particle size and salinity on the SDZ adsorption were examined in this study as well. The results showed that particle size has a strong relationship to adsorption capacity. Meanwhile, high salinity tends to inhibit the adsorption capacity, as the presence of salts might change the physicochemical properties of the sediments. It shall be noted that only inorganic components were used to represent the marine sediments, and the effect of organics was not considered in the present study. It was also found that, for fine sands, the adsorption amount may not increase with the Reynolds number, which deserves a deeper investigation in the future study. In general, this study may help provide the basis to further understand the fate of antibiotics in the estuary and coastal environments. Additionally, as the hydrodynamic condition plays a significant role on the adsorption behavior, the antibiotic concentration in the water environment is expected to be lowered by enhancing the turbulence intensity.

Author Contributions: W.X.: Methodology, Investigation, Writing. J.X.: Writing and revision. J.S.: Conceptualization, Supervision, Writing—review and editing, Supervision. G.X.: Conceptualization, Supervision. All authors have read and agreed to the published version of the manuscript.

Funding: This research was funded by Shanghai Sailing Program (20YF1409700). And The APC was funded by Shanghai Sailing Program (20YF1409700).

Institutional Review Board Statement: Not applicable.

Informed Consent Statement: Not applicable.

Data Availability Statement: No data were used for the research described in the article.

Acknowledgments: This work was sponsored by the Shanghai Sailing Program (20YF1409700).

Conflicts of Interest: The authors declare no conflict of interest.

References

1. Lyu, J.; Chen, Y.; Zhang, L. Antibiotics in Drinking Water and Health Risks—China, 2017. *China CDC Weekly* **2020**, *223*, 413–417. [CrossRef]
2. Liu, C.; Tan, L.; Zhang, L.; Tian, W.; Ma, L. A Review of the Distribution of Antibiotics in Water in Different Regions of China and Current Antibiotic Degradation Pathways. *Front. Environ. Sci.* **2021**, *9*, 24. [CrossRef]
3. Manzetti, S.; Ghisi, R. The environmental release and fate of antibiotics. *Mar. Pollut. Bull.* **2014**, *79*, 7–15. [CrossRef] [PubMed]
4. Singh, R.; Singh, A.P.; Kumar, S.; Giri, B.S.; Kim, K.-H. Antibiotic resistance in major rivers in the world: A systematic review on occurrence, emergence, and management strategies. *J. Clean Prod.* **2019**, *234*, 1484–1505. [CrossRef]
5. Anh, H.Q.; Le, T.P.Q.; Da Le, N.; Lu, X.X.; Duong, T.T.; Garnier, J.; Rochelle-Newall, E.; Zhang, S.; Oh, N.-H.; Oeurng, C.; et al. Antibiotics in surface water of East and Southeast Asian countries: A focused review on contamination status, pollution sources, potential risks, and future perspectives. *Sci. Total Environ.* **2021**, *764*, 16. [CrossRef] [PubMed]
6. Liu, X.; Zhang, H.; Li, L.; Fu, C.; Tu, C.; Huang, Y.; Wu, L.; Tang, J.; Luo, Y.; Christie, P. Levels, distributions and sources of veterinary antibiotics in the sediments of the Bohai Sea in China and surrounding estuaries. *Mar. Pollut. Bull.* **2016**, *1091*, 597–602. [CrossRef]
7. Ma, N.; Tong, L.; Li, Y.; Yang, C.; Tan, Q.; He, J. Distribution of antibiotics in lake water-groundwater-Sediment system in Chenhu Lake area. *Environ. Res.* **2022**, *204*, 9. [CrossRef] [PubMed]
8. Yin, J.; Gu, S.; Ke, H.; Shang, M.; Dong, J.; Li, D.; Xie, H.; Feng, R. Impact of anthropogenic activity on antibiotic behaviors in coastal waters. *Ecol. Indic.* **2022**, *144*, 8. [CrossRef]
9. Li, J.; Zhang, H. Factors influencing adsorption and desorption of trimethoprim on marine sediments: Mechanisms and kinetics. *Environ. Sci. Pollut. Res.* **2017**, *24*, 21929–21937. [CrossRef]
10. Doretto, K.M.; Rath, S. Sorption of sulfadiazine on Brazilian soils. *Chemosphere* **2013**, *90*, 2027–2034. [CrossRef]
11. Jara, B.; Srain, B.M.; Aranda, M.; Fernández, C.; Pantoja-Gutiérrez, S.; Méjanelle, L. Water-sediment partitioning of flumequine and florfenicol, two antibiotics used in salmon aquaculture in Chile. *Mar. Pollut. Bull.* **2022**, *177*, 7. [CrossRef] [PubMed]
12. Li, J.; Zhang, H. Adsorption-desorption of oxytetracycline on marine sediments: Kinetics and influencing factors. *Chemosphere* **2016**, *164*, 156–163. [CrossRef] [PubMed]
13. Liao, Q.; Huang, Z.; Li, S.; Wang, Y.; Liu, Y.; Luo, R.; Shang, J. Effects of wind-wave disturbances on adsorption and desorption of tetracycline and sulfadimidine in water-sediment systems. *Environ. Sci. Pollut. Res.* **2018**, *2523*, 22561–22570. [CrossRef]
14. Li, S.; Huang, Z.; Wang, Y.; Liu, Y.-Q.; Luo, R.; Shang, J.-G.; Liao, Q.-J. Migration of two antibiotics during resuspension under simulated wind-wave disturbances in a water-sediment system. *Chemosphere* **2018**, *192*, 234–243. [CrossRef]
15. Li, Y.; Tang, C.; Wang, J.; Acharya, K.; Du, W.; Gao, X.; Luo, L.; Li, H.; Dai, S.; Mercy, J.; et al. Effect of wave-current interactions on sediment resuspension in large shallow Lake Taihu, China. *Environ. Sci. Pollut. Res.* **2017**, *244*, 4029–4039. [CrossRef]
16. Xu, W.H.; Zhang, G.; Wai, O.W.; Zou, S.C.; Li, X.D. Transport and adsorption of antibiotics by marine sediments in a dynamic environment. *J. Soils Sediments* **2009**, *94*, 364–373. [CrossRef]
17. Gardner, J.; Tatterson, G. Characterization of mixing in shaker table containers. *Biotechnol. Bioeng.* **1992**, *39*(7), 794–797. [CrossRef]
18. Li, Y.; Ducci, A.; Micheletti, M. Study on mixing characteristics in shaken microwell systems. *Biochem. Eng. J.* **2020**, *153*, 10. [CrossRef]
19. Ndonga, M.; Tatterson, G. Characterization of mixing in flat-bottomed spherical flasks agitated with magnetic stirrers. *Chem. Eng. Commun* **2006**, *193*, 1414–1421. [CrossRef]
20. Kim, C.L.; Oh, J.M. Effect of Particle Size of Sediment on Adsorption of Fluoride. *Korean J. Ecol. Environ.* **2016**, *494*, 289–295. [CrossRef]
21. Wu, M.; Zhao, S.; Jing, R.; Shao, Y.; Liu, X.; Lv, F.; Hu, X.; Zhang, Q.; Meng, Z.; Liu, A. Competitive adsorption of antibiotic tetracycline and ciprofloxacin on montmorillonite. *Appl. Clay Sci.* **2019**, *180*, 7. [CrossRef]
22. Bao, L.I.; Qiushi, S.H.E.N.; Chunyi, S.U.N.; Guosheng, H.E.; Yang, L.I.U. Simulation of dynamic migration rules of Hg under different winds and waves in sediments of Nanyang Lake area, Nansi Lake, China. *Environ. Chem.* **2022**, *414*, 1356–1366.

23. Aminot, Y.; Fuster, L.; Pardon, P.; Le Menach, K.; Budzinski, H. Suspended solids moderate the degradation and sorption of waste water-derived pharmaceuticals in estuarine waters. *Sci. Total Environ.* **2018**, *612*, 39–48. [CrossRef]
24. Bulut, Y.; Aydin, H. A kinetics and thermodynamics study of methylene blue adsorption on wheat shells. *Desalination* **2006**, *194*, 259–267. [CrossRef]
25. Kato, Y.; Hiraoka, S.; Tada, Y.; Hirose, K.; Büchs, J. Mixing performance of a reciprocally shaking vessel. *J. Chem. Eng. Jpn.* **2003**, *366*, 663–667. [CrossRef]
26. Zhang, B.; Chen, J.; Wang, C.; Wang, P.; Cui, G.; Zhang, J.; Hu, Y.; Gao, H. Insight into different adsorption behaviors of two fluoroquinolone antibiotics by sediment aggregation fractions. *Environ. Sci. Pollut. Res.* **2022**, *30*, 24329–24343. [CrossRef]
27. Akcay, G.; Kilinc, E.; Akcay, M. The equilibrium and kinetics studies of flurbiprofen adsorption onto tetrabutylammonium montmorillonite (TBAM). *Colloid Surf. A-Physicochem. Eng. Asp.* **2009**, *3351–3353*, 189–193. [CrossRef]
28. Bansal, O.P. Thermodynamics of Equilibrium Adsorption of Antibiotics by Clay Minerals and Humic Acid-Clay Complexes. *Natl. Acad. Sci. Lett.-India* **2012**, *352*, 109–114. [CrossRef]
29. Zhong, Z.; Xu, J.; Zhang, Y.; Li, L.; Guo, C.; He, Y.; Fan, W.; Zhang, B. Adsorption of sulfonamides on lake sediments. *Front. Environ. Sci. Eng.* **2013**, *7*, 518–525. [CrossRef]
30. Wang, X.; Chen, A.; Chen, B.; Wang, L. Adsorption of phenol and bisphenol A on river sediments: Effects of particle size, humic acid, pH and temperature. *Ecotoxicol. Environ. Safety* **2020**, *204*, 8. [CrossRef]
31. Buyang, S.; Yi, Q.; Cui, H.; Wan, K.; Zhang, S. Distribution and adsorption of metals on different particle size fractions of sediments in a hydrodynamically disturbed canal. *Sci. Total Environ.* **2019**, *670*, 654–661. [CrossRef]
32. Kim, Y.; Son, Y.; Bae, S.; Kim, T.H.; Hwang, Y. Particle size and interlayer anion effect on chromate adsorption by MgAl-layered double hydroxide. *Appl. Clay Sci.* **2022**, *225*, 11. [CrossRef]
33. Zhao, P.; Zhao, Y.; Cui, L.; Tian, Y.; Zhang, Z.; Zhu, Q.; Zhao, W. Multiple antibiotics distribution in drinking water and their co-adsorption behaviors by different size fractions of natural particles. *Sci. Total Environ.* **2021**, *775*, 9. [CrossRef] [PubMed]
34. Yin, C.; Pan, C.-G.; Xiao, S.-K.; Wu, Q.; Tan, H.-M.; Yu, K. Insights into the effects of salinity on the sorption and desorption of legacy and emerging per-and polyfluoroalkyl substances (PFASs) on marine sediments. *Environ. Pollut.* **2022**, *300*, 9. [CrossRef]
35. Zhang, W.; He, Y.; Zhang, Q.; Meng, Y.; Liu, T.; Meng, W.; Zuo, Y.; Fan, H. Study on the Effect of Salinity and Water Content on CBM Adsorption/Desorption Characteristics of Coal Reservoir in Baode Block. *Geofluids* **2022**, *2022*, 9. [CrossRef]
36. Zhou, J.; Mao, Q.; Luo, K.H. Effects of Moisture and Salinity on Methane Adsorption in Kerogen: A Molecular Simulation Study. *Energy Fuels* **2019**, *336*, 5368–5376. [CrossRef]
37. Wang, S.S.; Xue, N.N.; Li, W.F.; Zhang, D.Y.; Pan, X.L.; Luo, Y.M. Selectively enrichment of antibiotics and ARGs by microplastics in river, estuary and marine waters. *Sci. Total Environ.* **2020**, *708*, 11. [CrossRef]